

Growth rate and morphology for ceramic films by pulsed-MOCVD

Susan Krumdieck*, Rishi Raj

Department of Mechanical Engineering, University of Colorado at Boulder, Campus Box 427, Boulder, CO 80309, USA

Received 23 May 2000; received in revised form 25 February 2001; accepted 6 March 2001

Abstract

Titania films were deposited on nickel substrates from a dilute solution of titanium isopropoxide (TTIP) in toluene in order to study the growth rate and degree of microstructure control attainable with a metalorganic chemical vapor deposition system called pulsed-MOCVD. This novel system employs pulsed liquid injection with ultrasonic atomization to deliver the precursor to the low-pressure reactor. The film growth rate was studied as a function of temperature and precursor injection rate. An Arrhenius behavior was evident for susceptor temperatures below 500°C. At higher temperatures, the growth rate was nearly equal to the injection rate. Films $45 \pm 0.1\text{-}\mu\text{m}$ thick were deposited at rates of up to $0.5 \pm 0.008\ \mu\text{m}/\text{min}$. Two methods were employed for measurement of film growth rate, direct in situ observation of color-fringe evolution and calculation from final film thickness measurements using an optical microscope. The influence of deposition parameters on morphology was studied. The microstructure was characterized using optical and scanning electron microscopy (SEM) and X-ray diffraction (XRD). At temperatures below 500°C the film was dense with small equiaxed crystals. At higher temperatures films were textured and columnar. With the combination of high injection rate and high temperature, fully dense oriented films were produced. © 2001 Published by Elsevier Science B.V.

Keywords: [C] Metalorganic chemical vapor deposition; [D] Titanium oxide; [C] Pulsed chemical vapor deposition; [C] Liquid injection; [D] Ceramic films

1. Introduction

Films of metal oxides have a wide range of application from electronics and sensors to optical, refractory, wear and corrosion-resistant coatings. In the current study, we were interested in application of the pulsed-MOCVD system for production of protective ceramic coatings on metal parts. Given the low thermal conductivity and high melting temperature of ceramics, it is easy to see the attraction of a ceramic coating on a

metal part which is exposed to high temperatures. Thermal barrier coatings (TBCs) are utilized to increase the thermal efficiency and performance of gas turbines by providing thermal and erosion protection of the metal blades. The performance of TBCs depends greatly on the microstructure of the film [1]. In order to compensate for the mismatch in thermal expansion between metal and ceramic, the film must have a columnar microstructure, with grain boundaries perpendicular to the metal surface. The coating must also be relatively thick ($> 50\ \mu\text{m}$) to provide adequate thermal protection [2].

The pulsed-MOCVD system has been employed in previous studies to produce heteroepitaxial LiTaO_3 [3] and TiO_2 [4] on sapphire substrates. These studies demonstrated that a metal alkoxide precursor solution

* Corresponding author present address: Department of Mechanical Engineering, University of Canterbury, P.B. 4800, Christchurch, New Zealand; Tel.: +64-3-364-9878; fax: +64-3-364-6078.

E-mail address: s.krumdieck@mech.canterbury.ac.nz (S. Krumdieck).

in a volatile solvent could be injected into a low-pressure reactor using ultrasonic atomization to produce a metal oxide film on a heated substrate. Alkoxide precursors, such as the titanium tetra isopropoxide, (TTIP) used in this study, are air- and moisture-sensitive and require an inert atmosphere for handling. TTIP decomposes into solid metal oxide (TiO_2), with water and isopropanol as vapor products [5]. An ultrasonic nozzle is needed to produce small droplets which vaporize rapidly. Without the nozzle, the film growth rate was limited by the precursor evaporation rate.

An effective pulsing mechanism for the precursor supply was recently developed, resulting in the unique operating regime of pulsed-MOCVD. Two motivating factors for this research are the improved process control over conventional atmospheric pressure CVD and the high growth rates compared to constant flow low-pressure CVD. The pulsed-MOCVD process replaces the carrier gas and bubbler delivery system with pulsed liquid delivery and ultrasonic atomization. One research group has recently reported improved process control using liquid injection for low-pressure tantalum pentoxide deposition from a metalorganic precursor [6]. Other researchers have found direct liquid injection advantageous for atmospheric-pressure MOCVD of doped alumina [7] and ferroelectric thin films [8]. The relative advantages and disadvantages of low-pressure and atmospheric-pressure CVD are well known [9]. Pulsed-MOCVD operates, alternately, between these two regimes with a time constant of less than 10 s. The liquid pulse is injected into the reactor at low-pressure (100–300 Pa) and rapidly vaporized, providing uniform concentration of the precursor at a higher pressure (1600–3200 Pa). Within 10 s, the typical pulse period, the reactor is pumped back down to the low pressure. We have observed that the pulsing action provides several benefits including even coverage, relatively fast growth rates, low cooling rates of the deposition surface, and low contamination in the film, as the products are actively removed.

The goal of this research was to determine the growth rate and characterize the film morphology throughout the range of temperature (400–700°C) and injection rate, which is a combination of precursor molar concentration (1.06–6.11%) and liquid flow rate (251–1005 $\mu\text{l}/\text{min}$). The growth rate was found to exhibit the expected Arrhenius behavior at low temperatures, then becoming almost constant at higher temperatures. At higher temperatures the deposition rate (moles/min) is so close to the injection rate (moles/min) that we suggest that the rate-controlling step is the precursor injection rate, rather than the precursor diffusion rate commonly encountered in atmospheric pressure CVD. A range of morphologies was observed depending on the relative rates of precursor supply, precursor decomposition on the heated surface

and crystal growth. Columnar microstructure films were obtained for temperatures above 500°C and precursor concentration above 2% M.

2. Experiments

2.1. Experimental set-up

Fig. 1 shows a schematic drawing of the vertical cold-wall apparatus used in this study. Typically, three samples of nickel of approximately 1 mm thickness and 1 cm^2 surface area are clamped to the susceptor. A halogen lamp encased in heat shielding heats the susceptor. The deposition temperature is measured by a thermocouple inserted into a cavity in the susceptor and controlled by a Eurotherm proportional controller. The reactor pressure is supplied by a rotary vacuum pump and exhausted through a liquid nitrogen trap.

Each pulse cycle delivers an exact amount of liquid precursor solution to the reactor through the ultrasonic nozzle. The pulsed liquid injection is accomplished by controlling the flow through three solenoid valves with the LabView software on a personal computer. Valve A in Fig. 1 controls the liquid source supply. The solvent is used only to flush the lines and nozzle after each experiment.

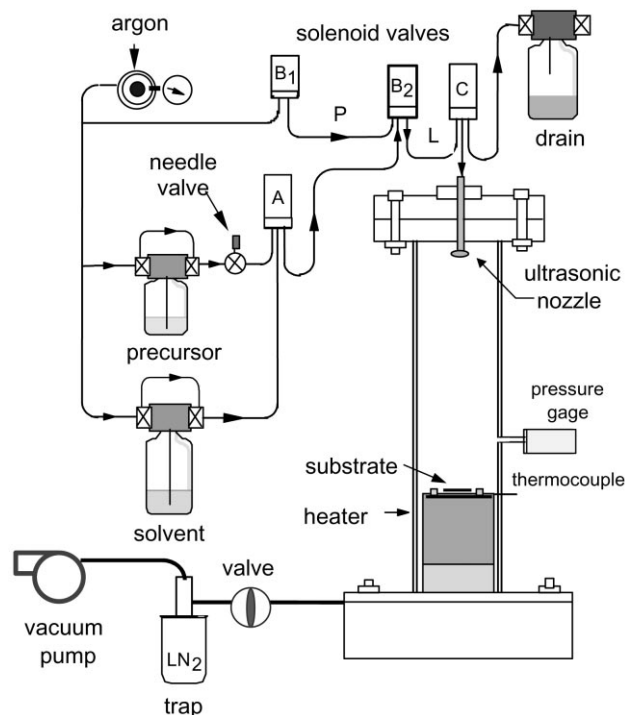


Fig. 1. Schematic representation of the pulsed-MOCVD experimental apparatus. The timed operation of the valves results in the pressurized argon shot in tube length P pushing the liquid precursor shot in tube L into the reactor through the ultrasonic nozzle at regular pulse intervals.

The operator specifies the pulse period and the total number of pulses in LabView. Valves B_1 and B_2 operate to isolate a shot of argon in tube length P while the precursor is flowing through valve C with slight overflow to the drain. In the injection stage of the pulse cycle, the argon shot pushes the precursor volume in tube length L through the ultrasonic nozzle into the reactor. The pulse volume is injected into the reactor and vaporized virtually instantaneously. The length of tube L and the internal volume of valves B_2 and C determine the pulse volume. The small (18 μm median diameter) [10] droplets from the ultrasonic nozzle evaporate quickly producing a pressure pulse, P_{max} . The reactor is then pumped down to P_{min} resulting in the pressure profile approximated by:

$$P(t) = P_{\text{min}} + \Delta P \exp\left(-\frac{t}{\tau_p}\right) \quad (1)$$

Where $\Delta P = (P_{\text{max}} - P_{\text{min}})$, t is the time during the pulse, and τ_p is the pump constant which was experimentally determined by fitting the exponential function to the measured pressure profile. Pressure was measured using a Varian Convectograph gage with an accuracy of 2% in the range of $0.1\text{--}10^5$ Pa.

The precursor injection rate is further controlled by adjusting the concentration of TTIP [$\text{Ti}(\text{OC}_3\text{H}_7)_4$ Alfa AESAR N35794] in the precursor solution. Solutions of a high volatility solvent, toluene (Sigma Aldrich 99.8% PRA grade), and up to 20% volume of TTIP are prepared in a controlled atmosphere dry glove box, loaded into the precursor supply bottle, sealed, and installed into the liquid supply system. The injection rate of TTIP in moles per pulse can be calculated by:

$$\text{Inj} = \frac{c_{\text{vol}} v_p \rho_{\text{TTIP}}}{\text{Mw}} \quad (2)$$

Where c_{vol} is the volume concentration of TTIP in solvent, v_p is the volume of solution injected per pulse [$\mu\text{l}/\text{pulse}$], ρ_{TTIP} is the density of TTIP [g/cm^3], and Mw is the molecular weight of $\text{Ti}(\text{OC}_3\text{H}_7)_4$.

2.2. Experimental method

Up to three nickel substrates were coated during each experiment, providing several samples for analysis at each set of deposition conditions. Typically, one sample was examined in cross-section with the optical microscope, one on the surface with SEM and EDS, and one was used for XRD analysis.

The growth rate of TiO_2 from TTIP was measured as a function of temperature for each set of precursor concentration and pulse rate conditions. Growth rate measurements from over 80 experiments were accomplished by two methods, observation of in situ color

fringe shift rate and calculation from post-deposition thickness measurement. The color fringe method involves timing the evolution of the color of the growing film [11]. Each color, in the case of TiO_2 alternating red and green, represents a multiple of the thickness of a single colored layer, which was measured with an ellipsometer. Color shift growth rate measurements have an error of $\pm 0.004 \mu\text{m}/\text{min}$. The overall average growth rate for the deposition was determined from run time and film thickness measured by stage micrometer on an optical microscope with accuracy of $\pm 0.1 \mu\text{m}$. The two measurement methods for growth rate were in good agreement ($R = 99$).

The morphology of the growing film and the coverage were observed over the range of deposition temperature and injection rate. Representative films from each set of operating conditions were visually examined to characterize the morphology, and analyzed with XRD to determine phase and texture. Samples were mounted side-on in resin, ground and polished, then observed with optical microscope ($20\text{--}150\times$ magnification). Carbon contamination for samples deposited in the optimal temperature range ($525\text{--}575^\circ\text{C}$) was measured with energy dispersive detector (EDS) with a detection limit of 0.5% weight of carbon. Table 1 provides the variable range for the matrix of experiments. The combination of precursor concentration and pulse rate according to Eq. (2) gives a range of precursor injection rate from 3.9 to 20.8×10^{-3} moles/min.

3. Results

3.1. Effects of temperature and injection rate on growth rate

The film deposition rate is controlled at lower temperatures (below 500°C) by the decomposition reaction rate, and at higher temperature by the precursor supply rate. Fig. 2 shows an Arrhenius plot of the growth rate as a function of temperature for several different TTIP concentrations but constant pulse rate. The growth rate at low temperature can be represented by a second order rate equation:

$$GR(T) = A \exp\left[\frac{-E_A}{RT}\right] \quad (3)$$

Where A is the rate constant, E_A is the activation energy, R is the gas constant and T is the surface temperature. The activation energy can be estimated from the slope of the growth rate with temperature in the low temperature region, $E_A = 95 \pm 5 \text{ kJ/g per mole}$ [12].

The growth rate becomes limited by the precursor supply rate in the temperature range between 550 and

Table 1
Matrix of experimental conditions for 80 deposition experiments

	Temperature variable	Concentration variable	Pulse rate variable
Precursor source temperature	23°C	23–80°C	23°C
Deposition temperature, T_s	400–700°C	550°C	550°C
TTIP molar concentration, c_{mo}	1.8%	1.06–6.11%	1.06%
Pulse period, t_p	10 s	10 s	4–16 s
Volumetric flow rate	402 $\mu\text{l}/\text{min}$	402 $\mu\text{l}/\text{min}$	251–1005 $\mu\text{l}/\text{min}$
Reactor peak pulse pressure	1600 Pa	1600 Pa	1600–3200 Pa
Reactor minimum pulse pressure	100 Pa	100 Pa	100–300 Pa
Deposition time	30–90 min	10–60 min	10–20 min
<i>Reactor dimensions:</i>			
Median droplet diameter	18 μm		
Reactor diameter	6 cm		
Susceptor diameter	4.5 cm		
Nozzle tip–substrate distance	18.5 cm		

650°C. At higher deposition temperatures, in the range above 600°C, homogeneous vapor-phase decomposition of the precursor due to convective and radiative heating of the vapor leads to powder deposition of anatase phase TiO_2 . This results in a decreasing rutile film growth rate with increasing temperature.

The growth rate increases linearly with precursor concentration up to 4% M, then remains constant with increased concentration, and decreases with increased pulse rate. As seen in Fig. 2, for high temperature depositions the growth rate increases directly with increased injection rate. The system performance is constrained by the concentration and pulse rate. TTIP has a much lower volatility than toluene. At higher concentrations, the reactor walls become coated with the precursor as droplets that do not evaporate before

impacting. The growth rate actually decreases for concentrations above 5% M. For much the same reasons, the growth rate decreases if the pulse rate is increased because the operating pressure is effectively increased and more precursor impacts on the reactor walls before evaporating. The growth rate at high injection rate becomes limited by the precursor evaporation rate.

Deposition efficiency, expressed as moles of oxide film/moles of precursor injected, was determined from measurements of final film thickness, h , and from the molar injection rate times the number of pulses, Inj_T [12]:

$$\eta = \frac{h \cdot \rho_{\text{TiO}_2}}{\text{Mw}_{\text{TiO}_2} \cdot \text{Inj}_T} \quad (4)$$

The density of rutile phase TiO_2 is $\rho_{\text{TiO}_2} = 4.26 \text{ g}/\text{cm}^3$, and the molecular weight is $\text{Mw} = 79.90 \text{ g}/\text{g mole}$. The highest efficiency rutile deposition $90 \pm 5\%$ was in the temperature range of 575–600°C, for any precursor concentration below 5% M, and for pulse rate of 10 s/pulse. This high efficiency is attributed to two main factors: (1) the high degree of mixing in the reactor due to the pulsing atomization; and (2) the operation without carrier gas. The beneficial effect of the pulsed injection delivery system is that a concentration boundary layer is not present when the precursor concentration is the highest, at the beginning of the pulse [13].

3.2. Effects of temperature and injection rate on morphology

The film morphology is determined by the relative rates of precursor vapor arrival, decomposition reaction, surface diffusion, and lattice incorporation [14].

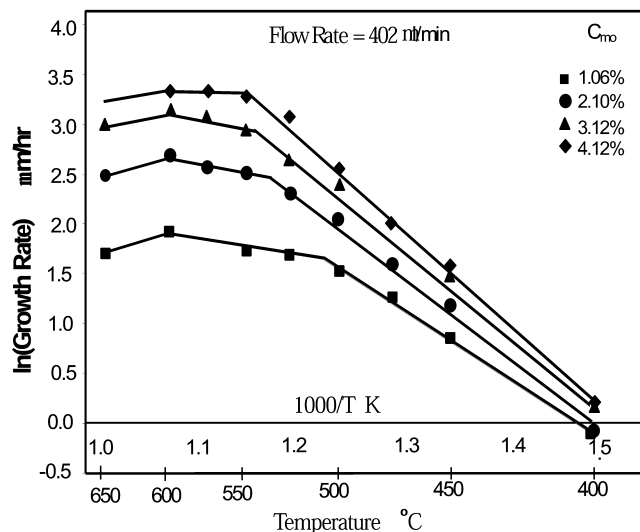


Fig. 2. Arrhenius plot of experimental growth rate data for a range of precursor concentration.

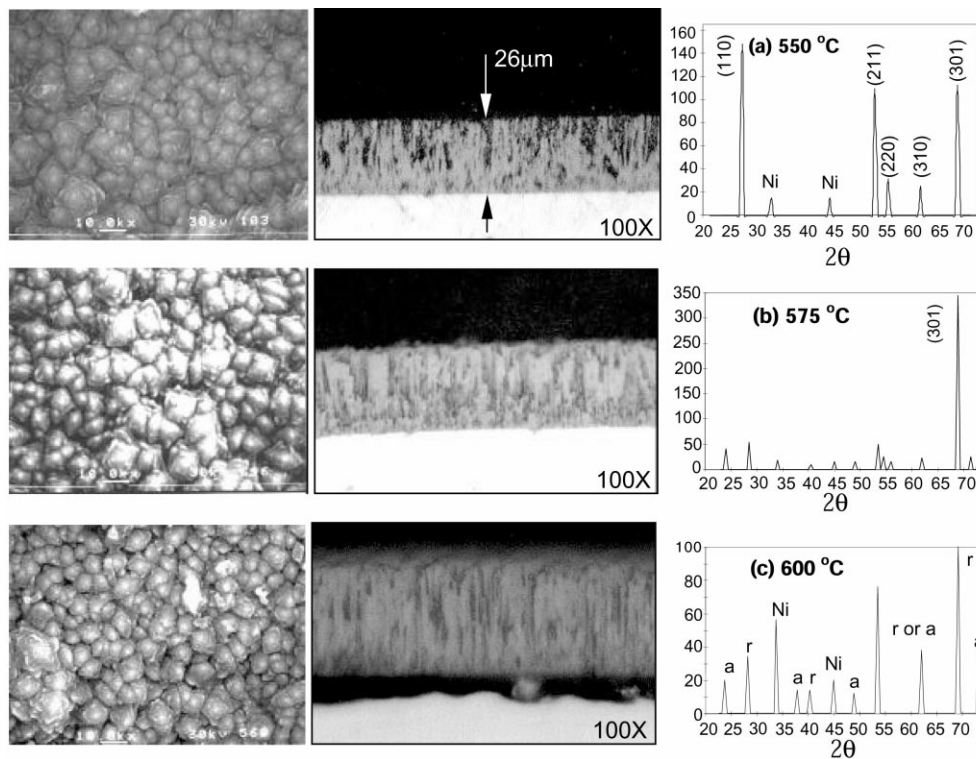


Fig. 3. Surface and cross-sectional micrographs and corresponding XRD patterns of TiO_2 films grown on nickel at three different temperatures: (a) 550°C only rutile phase present; (b) 575°C highly oriented rutile phase; and (c) 600°C rutile and anatase phase present. All depositions were at 1.8% M concentration of TTIP precursor and 10 s pulse cycle.

At low temperatures the microstructure is nearly equiaxed and the texture shows very little preferred orientation. However, as temperature increases, the energy for surface diffusion increases, as does the growth rate, resulting in more rapid lattice incorporation on low energy crystal planes. This growth produces a columnar microstructure with (301) texture, as seen in Fig. 3.

At temperatures above 600°C , the XRD pattern shows a high degree of orientation and evidence of the presence of the anatase phase of TiO_2 . This phase is formed at lower temperatures than the rutile phase, providing evidence that the anatase phase is formed by gas phase decomposition as the vapor is heated prior to precursor adsorption. The anatase deposits were visible with optical microscope as white powder deposits on the columnar film surface.

The density, texture and morphology are functions of the precursor injection rate. All of the films grown at very low precursor concentration, below 1% M, had an equiaxed, granular structure, which showed no porosity on a polished surface. Deposition between 1.4 and 4% molar concentration, exhibited some degree of porosity (observable void size of $0.001\ \mu\text{m}$). Segmentation of the columnar crystallites and voids along the grain boundaries are evident in the microstructure of films grown at 550°C for precursor solution concentration below 5% M. The films grown at 550°C and 5.3% M precursor

concentration showed a very high degree of orientation, indicating columnar structure. However, the segmentation and voids were not apparent in the micrographs for these films as seen in Fig. 4. At higher concentrations, the deposition rate appears to outpace the surface diffusion rate and a prismatic columnar structure is evident. This structure is less dense than the oriented columnar structure, with definite segmentation and voids between crystallites.

The experimental deposition of TiO_2 by pulsed-MOCVD produced morphologies from fine-grained equiaxed to columnar, depending on the growth conditions. The resulting microstructures followed the patterns expected from crystal growth theory [15]. Low growth rate, either due to low temperature or low injection rate, produced a fine-grained equiaxed structure. Moderate growth rates produced columnar microstructure with segmentation along grain boundaries. High growth rates produced fully dense, highly oriented columnar microstructure. Extremely high growth rates produced the prismatic columnar microstructure with large voids between crystallites. The degree of control of the substrate temperature and precursor injection rate afforded by the pulsed-MOCVD system, indicate that the process can reliably produce an oxide layer with the desired microstructure. Fig. 5 shows a microstructural process map for all experiments.

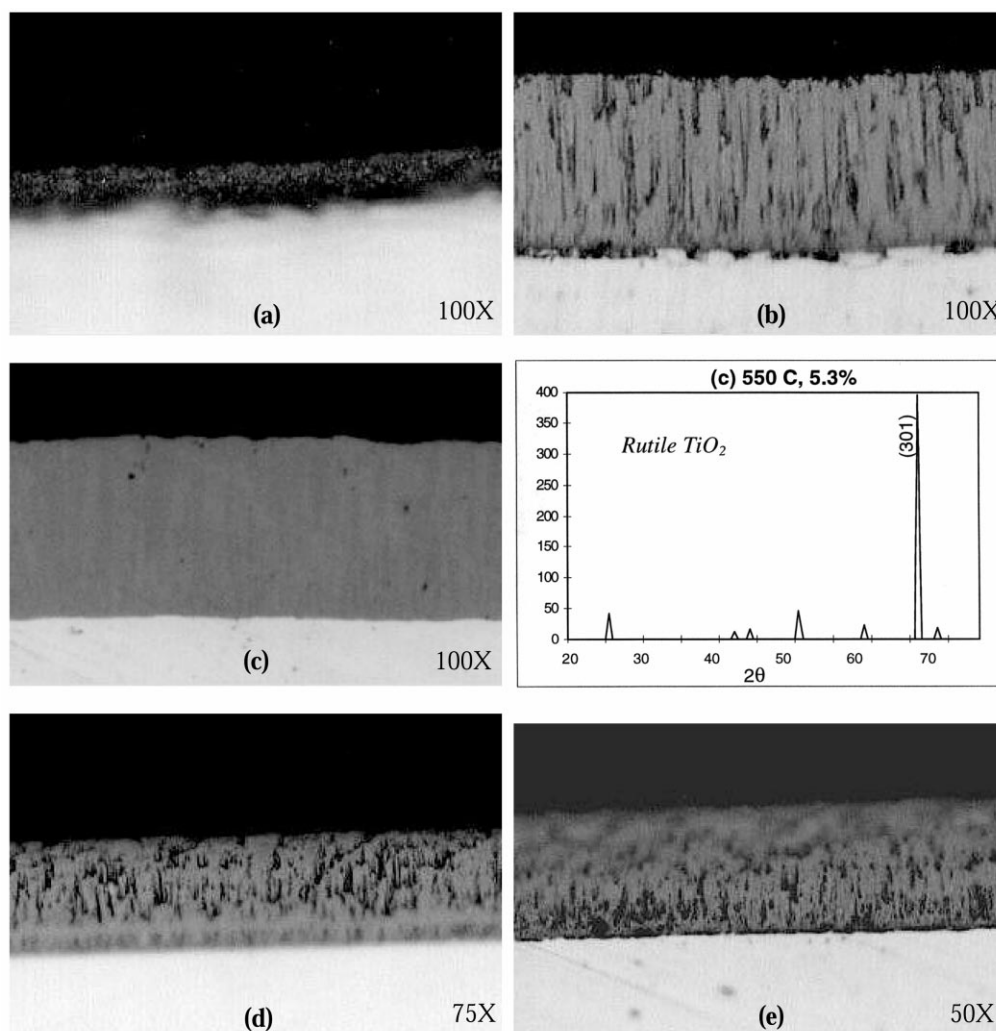


Fig. 4. Cross-sectional micrographs of TiO_2 films grown on nickel at four different precursor molar concentrations of $\text{Ti}(\text{OPr})_4$: (a) 0.71%; (b) 3.5%; (c) 5.3% with XRD pattern showing high degree of texture; (d) 6.11%; and (e) 7.4%, all at 550°C deposition temperature and 10 s pulse cycle.

3.3. Coverage and carbon contamination

The uniformity of the film thickness was found to depend only on the uniform temperature of the substrate and not on the position relative to reactor flow. The substrate heater used in these experiments is admittedly not of an optimally reliable design. Observing the film color fringes, it is clear to see when a problem with the heater exists and the susceptor is not heated uniformly. That said, films deposited under isothermal conditions had no measurable thickness variation ($\pm 0.1 \mu\text{m}$) as a function of the radial position in the reactor. The uniformity of the coating on flat substrates was $99.5 \pm 0.5\%$ for coating thickness in the 20- μm range. The layers were also observed to be conformal, that is the thickness did not change over bumps on the substrate or around the substrate edge. Uniform, conformal coverage is expected in low pressure CVD [16].

The carbon contamination in films deposited at temperatures below 575°C was below the detection limit of the EDS equipment (0.5% wt.). At temperatures above 600°C, some black coating was observed on the reactor walls and around the base of the heater. However, EDS analysis of a film deposited at 600°C was found to have less than 4% weight of carbon.

4. Conclusion

The goal of the project was to assess the potential of the pulsed-MOCVD process for deposition of ceramic coatings on metal. Rutile phase TiO_2 films were grown on nickel substrates as a model system. The metalorganic precursor TTIP in a dilute solution of toluene was directly injected via a pulsing mechanism, into a low-pressure cold wall reactor through an ultrasonic atomizer. The film growth rate and morphology were

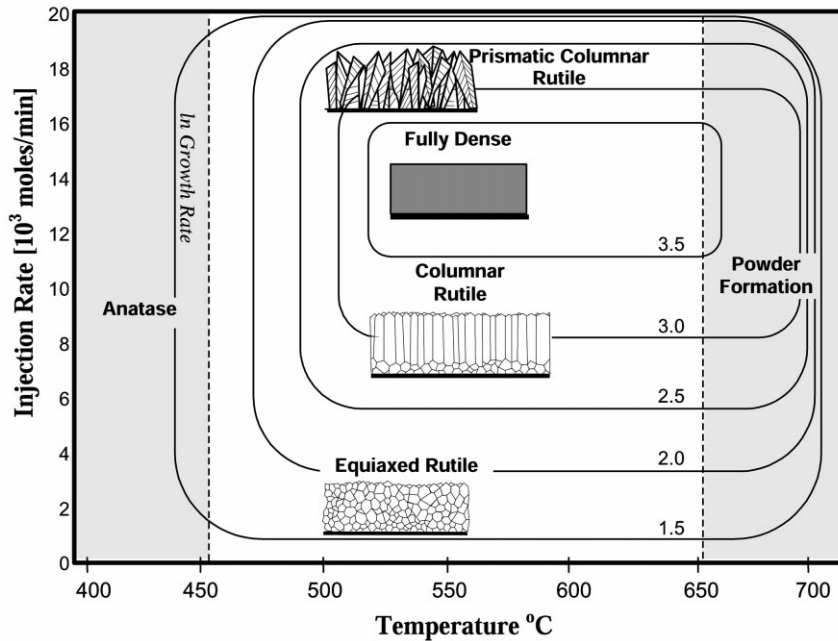


Fig. 5. Microstructure and phase processing map for pulsed-MOCVD of TiO_2 from TTIP precursor over the range of deposition conditions.

investigated over the operational range of the two process parameters, substrate temperature and molar injection rate.

The growth rate behavior as a function of temperature was found to exhibit the expected behavior for CVD processes. At low temperatures the growth rate increases exponentially with temperature, then becomes almost constant with increased temperature as the rate-controlling step becomes the precursor injection rate. Growth rates of up to $0.5 \pm 0.008 \mu\text{m}/\text{min}$ were achieved at conversion efficiencies exceeding $85 \pm 5\%$. The fact that there is a brief period of high precursor concentration, results in relatively high growth rates for a low pressure process.

The microstructure of the film was effectively controlled through the deposition conditions. Segmented columnar microstructure coatings up to $40 \pm 0.1 \mu\text{m}$ in thickness were grown at temperatures between 525 and 600°C . Such coatings have potential applications as thermal barrier coatings. Fully dense films from 4 to $45\text{-}\mu\text{m}$ thick were deposited in the same temperature range but with higher precursor injection rates. This type of layer would make a more effective environmental barrier coating and has the characteristics necessary for electronic applications, and for the electrolyte layer in solid oxide fuel cells. A high porosity prismatic microstructure resulted from very high injection rates. This high surface area and porosity would be useful on catalytic surfaces. Deposited films were found to have uniform coverage and no detectable carbon contamination (0.5% wt.) for deposition temperatures below 575°C .

The unsteady nature of the process gives rise to conversion efficiencies and microstructure control not normally encountered in conventional atmospheric pressure, steady flow CVD systems. The improvement in performance is attributed to the absence of concentration gradients in the reactor during the portion of the deposition cycle when precursor concentration is at a maximum.

Acknowledgements

The research was supported by the National Science Foundation under Grant No. DMI-9796114. Dr Krumdieck also received support from an ARCS Foundation Scholarship and an SAE Doctoral Scholars Award. The pulsed ultrasonic nozzle method was developed in collaboration with and contribution from Dr Harvey Berger, Sono-Tek Corporation, Milton, NY [17]. The authors also acknowledge the expert assistance of F. Luiszer with SEM and P. Boni with XRD analysis.

References

- [1] D.E. Wolfe, J. Singh, in: Y. Pauleau, P.B. Barna (Eds.), *Protective Coatings and Thin Films*, 1997, pp. 441–465
- [2] D.P. Stinton, T.M. Besmann, R.A. Lowden, *Ceram. Bull.* 67 (2) (1988) 31–37.
- [3] H. Xie, R. Raj, *Appl. Phys. Lett.* 63 (1993) 3146–3148.
- [4] V.A. Versteeg, C.T. Avedisian, R. Raj, *J. Am. Ceram. Soc.* 78 (10) (1995) 63–68.
- [5] C.P. Fictorie, J.F. Evans, W.L. Gladfelter, *J. Vac. Sci. Technol. A* 12 (4) (1994) 1108–1113.

